

Controllable Reversibility of an sp^2 to sp^3 Transition of a Single Wall Nanotube under the Manipulation of an AFM Tip: A Nanoscale Electromechanical Switch?

Lei Liu,¹ C. S. Jayanthi,¹ Meijie Tang,² S. Y. Wu,¹ Thomas W. Tomblor,³ Chongwu Zhou,³ Leo Alexseyev,³ Jing Kong,³ and Hongjie Dai³

¹Department of Physics, University of Louisville, Louisville, Kentucky 40292

²Physics Directorate, Lawrence Livermore Laboratory, Livermore, California 94551

³Department of Chemistry, Stanford University, Stanford, California 94305

(Received 28 December 1999)

A simulation of the deflection of a single wall nanotube under the manipulation of an atomic force microscope tip revealed the key feature characterizing the deformation at relatively small bending angles to be a reversible transition from sp^2 to sp^3 bonding configurations in the bending region, leading to a 2 orders of magnitude reduction in conductance consistent with our most recent experimental observation. A local analysis elucidating the underlying physics of the findings is also discussed.

PACS numbers: 72.80.Rj, 73.40.-c, 73.61.Wp

In recent years, there has been a concerted effort, both experimental [1,2] and theoretical [3–9], devoted to the study of the interplay between mechanical deformation and electrical properties of carbon nanotubes (NTs) because of the potential applications in the development of nano-electro-mechanical devices (NEMs). The experimental studies observed only relatively small changes in sample resistance for a NT under mechanical deformation unless the NT fractures or perturbations are made to the tube-metal contacts [2]. Theoretical calculations found that the electrical properties of bent single wall nanotubes (SWNTs) are insensitive to small bending angles (θ , the angle between the end of the tube and the unbent axis). Specifically, Nardelli and Bernholc [8] showed that, for a (5,5) metallic SWNT, no significant change in the conductance occurred for θ up to 24° and the conductance decreased by a factor of 2 at $\theta = 36^\circ$. Rochefort *et al.* [9] found that the conductance for a metallic (6,6) SWNT was essentially unchanged for θ up to 22.5° and decreased by a factor of ≤ 10 for large θ (up to 45°). Most recently, we conducted an experimental investigation of the effect of mechanical deformation on the electrical properties of SWNT, using an atomic force microscope (AFM) tip to reversibly deflect a suspended SWNT without changing the contact resistance [10]. The tips were made of silicon with radius of curvature in the range from a few to ~ 15 nm. In Fig. 1, we reproduce the schematic drawings of the experimental setup [10]. The SWNT bridging a pair of metal electrodes (20 nm thick Ti placed on top of the SWNT) was suspended across a trench (typically of 100–1000 nm wide and 175 nm deep) prefabricated in between the catalyst islands on a SiO_2/Si substrate [see Fig. 1(a)]. Placing an AFM tip above the center of the suspended SWNT, the sample stage containing the SWNT was moved upward and then retracted [see Fig. 1(b)]. The up-and-down cyclic movement was repeated many times while the AFM cantilever deflection and the resistance of the SWNT were simultaneously

recorded as a function of time. Our *in situ* measurements of the conductance found an *unexpected* decrease in conductance of 2 orders of magnitude when the AFM tip deflected the center of a suspended SWNT to a *seemingly small* bending angle ($\theta = 13^\circ$). We also found that the conductance and the structure recovered as the tip retracted. This controllable reversibility of the deformation-induced 2 orders of magnitude change in conductance clearly indicates the feasibility of utilizing this process in the design of NEMs.

Our experimental observation is obviously very different from the results of previous studies. We compare the relevant factors characterizing our experimental procedure with those defining previous theoretical studies. We find a

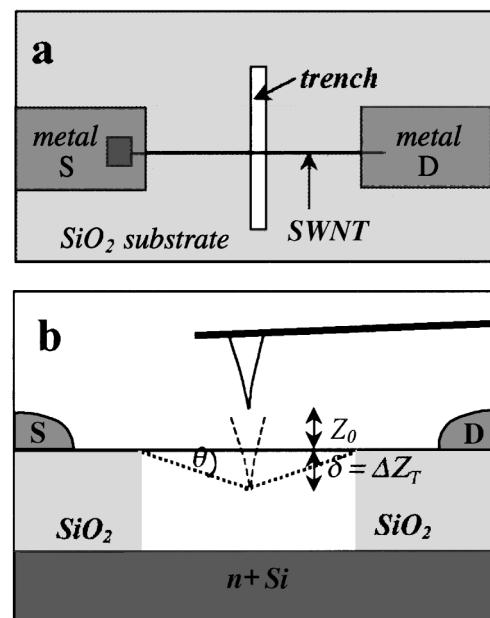


FIG. 1. (a) A schematic view of the experimental setup. (b) A schematic (side) view of the pushing-and-retracting action with respect to the AFM tip.

key factor which plays a prominent role in the experimental procedure yet it is missing in the theoretical considerations. This is the pushing-and-retracting action of the AFM tip as it is manipulated to induce the mechanical deformation on the SWNT. In previous theoretical studies [7–9], the bending of the SWNT was modeled by holding the ends of the SWNT at positions defining the angle of bending. This initial configuration was then allowed to relax to its equilibrium configuration while the ends were kept at the initial fixed positions. The equilibrium configuration of the bent SWNT obtained in this way, in particular in the neighborhood of the center of the SWNT, is certainly not expected to be able to model that of the bent SWNT obtained in our experiment under the pushing action of an AFM tip. This is because the pushing action of the AFM tip will give rise to a concentrated local strain in the section of the SWNT in the immediate neighborhood of the tip. Thus, to shed light on the physics behind the unexpected reduction in conductance by 2 orders of magnitude at a relatively small angle of deflection of $\theta = 13^\circ$, one must model the experimental procedure carefully by explicitly involving the AFM tip, in particular the pushing-and-retracting action of the tip. In this Letter, we report the results of our tight-binding simulations of the deformation of a SWNT under the pushing and retracting action of an AFM tip, and of our study of its underlying physics and consequences.

Since the SWNT sample in our experiment exhibits no appreciable change in conductance under various back-gate voltages and remains conducting at low temperatures, the sample tube is identified as a metallic (5,5) SWNT containing 960 carbon atoms ($l \approx 120 \text{ \AA}$) as our “sample.” The AFM tip was modeled by a capped (5,5) SWNT with 110 carbon atoms. The tip was first placed above the center of the suspended SWNT and then pushed downward vertically at a uniform speed in a continuous manner to deflect the SWNT. The molecular dynamics (MD) simulation of the continuous deflection of the SWNT was carried out at 300 K. Because of the size of the system under consideration, an order- N /nonorthogonal tight-binding MD [O(N)/NOTB-MD] scheme was used to carry out the simulation [11]. The NOTB Hamiltonian developed by Menon, Subbaswamy, and Sawtarie [12] was used in the calculation. This Hamiltonian is constructed in terms of s and p orbitals, and hence is equipped to take into account any effect associated with σ - π hybridization. To model the pushing action of the tip, the 50 atoms at the far end (from the sample) of the tip were held rigidly as a unit, and they were moved downward at a speed of 0.002 \AA/step (383 m/s with a time step of 0.522 fs , a speed which is actually about 2 orders of magnitude smaller than the thermal speed of atoms at 300 K). Forty atoms at each end of the suspended SWNT were held at their fixed positions during the simulation. The rest of the atoms, including the 60 atoms in the bottom portion of the tip (adjacent to the SWNT) and 880 atoms in the SWNT, were allowed to move under the

action of the atomic forces [calculated by the O(N)/NOTB scheme]. The deflection process went on until the bending angle θ reached 15° . To check the observed reversibility of the SWNT, the tip was then pulled back in the same manner. In Fig. 2, the equilibrium configurations of the system, i.e., the SWNT and the tip, during the pushing-and-retracting action of the tip are shown. These equilibrium configurations were obtained after the system was relaxed at the specified bending angle. The top four figures in the panel show the equilibrium configurations corresponding to $\theta = 0^\circ, 7^\circ, 11^\circ$, and 15° , respectively, as the tip pushes down on the SWNT. The bottom three figures give the configurations corresponding to $\theta = 11^\circ, 7^\circ$, and 0° during the retracting stage of the tip’s pushing-and-retracting cycle. It can be seen that, for $\theta = 7^\circ$, the deformation of the SWNT in the vicinity of the tip is basically elastic in nature. However, for $\theta \geq 11^\circ$, there is a noticeable

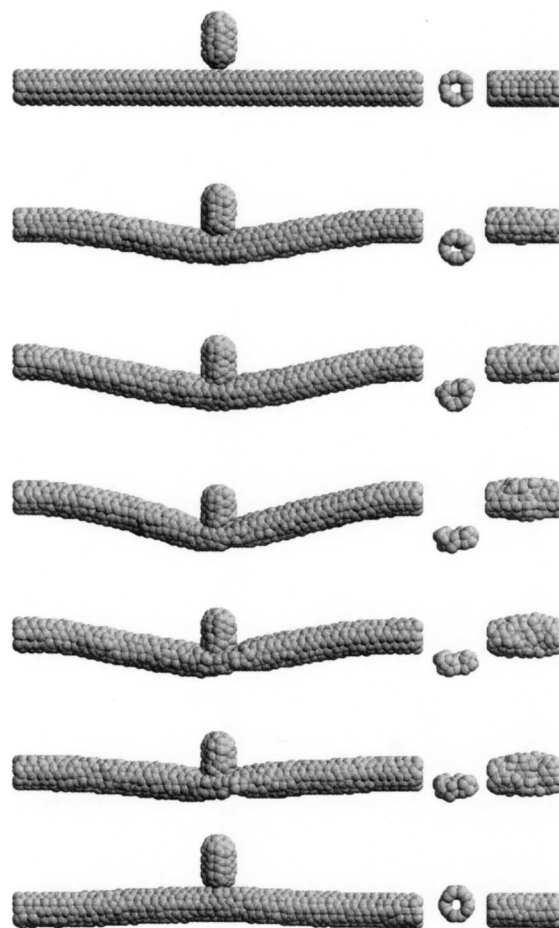


FIG. 2. Simulations of the deformation under the manipulation of an AFM tip. The top four figures show the equilibrium configurations corresponding to $\theta = 0^\circ, 7^\circ, 11^\circ$, and 15° , respectively, during the downward motion of the tip while the bottom three figures show the equilibrium configurations corresponding to $\theta = 11^\circ, 7^\circ$, and 0° , respectively, as the tip is being withdrawn. The accompanying figures in each case give the side view and the top view, respectively, of the bending region. θ is calculated by $\theta = \tan^{-1}(2\delta/l)$ where δ is defined in Fig. 1(b) and l is the suspended length of the SWNT.

change in the bonding configuration for the atoms in the central section of the SWNT in the proximity of the tip. Using either the distance or the bond charge criterion [13], one can determine the average number of bonds per atom in the central section of the SWNT. At $\theta = 11^\circ$, this number has already changed from 3 to 3.3 while at $\theta = 15^\circ$, this number has reached 3.6. This dramatic change in the average number of bonds per atom in the central section of the SWNT (near the tip) where the bend is located signifies that a change in the nature of bonding, namely, from a sp^2 to a sp^3 bonding, has occurred for atoms in the bending region. It should be noted that no such change had been observed even for a bending angle up to $\theta = 45^\circ$ in previous simulations where no concentrated local deformation was present in the SWNT. Since electrons in sp^3 bonding are localized, this change could bring about drastic change in the electric properties of the SWNT. The bottom three figures show that, as the tip was being withdrawn in a continuous manner from $\theta = 15^\circ$, the SWNT returns to its original unbent structure. This observation of reversibility of the SWNT under the manipulation of an AFM tip for small bending angles is consistent with the experimental observation. It indicates that while the system as a whole (the bent SWNT and the tip) is in its equilibrium configuration, the structure of the bent SWNT by itself, at least for $\theta \geq 11^\circ$, is very unstable. It exists entirely due to the anchoring of the tip near by. As the tip is pulled back, the extremely unstable structure of the bent SWNT immediately starts to recover from its precarious configuration, thus putting stress on the extra bond formed in the change from a sp^2 to sp^3 bonding configuration for the atoms in the central section of the SWNT. The stress eventually breaks the extra bond, and the SWNT returns to its unbent configuration as the tip pulls away.

We have also carried out a local analysis [13] of the bonding nature between carbon atoms and their neighbors in the bending region of the SWNT. Figure 3 shows that, as expected, there is a decrease in the bond charge per

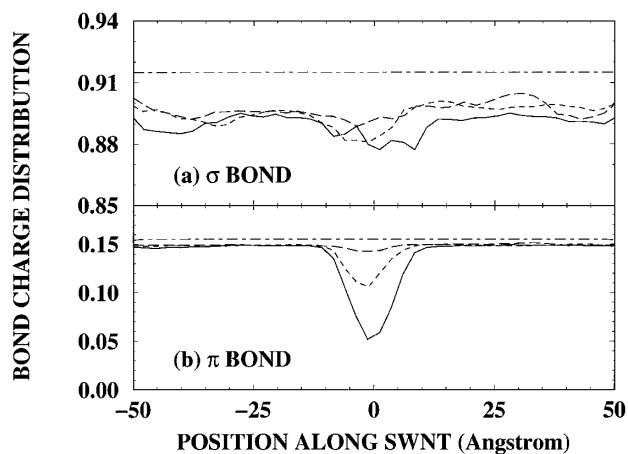


FIG. 3. Average bond charge per atom along the SWNT. The dot-dashed line corresponds to $\theta = 0^\circ$, the long-dashed line $\theta = 7^\circ$, the short-dashed line $\theta = 11^\circ$, and the solid line $\theta = 15^\circ$.

atom along the SWNT, a consequence of an increase in the average spacing between pairs of atoms as the tube is “stretched.” For atoms in the bending region, there is only a small percentage change in the electron number in the σ bonding, and this change is relatively insensitive to the bending angle. However, there is a substantial reduction in the electron number in the π bonding, and this reduction increases with increasing bending angle. Since the electrons in the $pp\pi$ bond are delocalized and therefore are mainly responsible for the conduction, a substantial reduction in the number of π electrons will cause a drastic decrease in the conductance. Hence, the experimentally observed reduction in the conductance of 2 orders of magnitude when the SWNT is bent from $\theta = 0^\circ$ to 13° might be attributable to the change in the bonding nature from the sp^2 to the sp^3 configuration due to the local deformation induced by the tip.

Thus we calculated the conductance of the SWNT by connecting it to two semi-infinite leads, left (L) and right (R). In our calculation, both leads are chosen to be the ideal (5,5) SWNTs. In this way, the conductance can be expressed as $G = \frac{2e^2}{h} \text{Tr}(\Gamma_L R_S^r \Gamma_R R_S^a)$ where $R_S^{a(r)}$ is the advanced (retarded) Green’s function of the sample (the bent NT) [14]. The advanced (retarded) Green’s function can be calculated by $R_S^{a(r)} = \{ES_S - h_S - \nu'_{SL} \Delta_L^{a(r)} \nu'_{LS} - \nu'_{SR} \Delta_R^{a(r)} \nu'_{RS}\}^{-1}$, with $\nu'_{SL(SR)} = ES_{SL(SR)} - \nu_{SL(SR)}$, h_S being the Hamiltonian of the bent NT (the sample), S_S the overlapping matrix of the sample, $S_{SL(SR)}$ the overlapping matrix between the sample and the left (right) lead, $\nu_{SL} (\nu_{SR})$ the coupling between the sample and the left (right) lead, and $\Delta_L^{a(r)} (\Delta_R^{a(r)})$ the advanced (retarded) Green’s function for the semi-infinite left (right) lead [15]. Since the leads are ideal semi-infinite (5,5) NT, we have $\Delta_L^{a(r)} = \Delta_R^{a(r)} = \{(E \pm i\varepsilon)S_0 - h_0\}^{-1}$ where h_0 and S_0 are the Hamiltonian and the overlapping matrix for the semi-infinite (5,5) NT, respectively [15]. The coupling term $\Gamma_{L(R)}$ can be expressed as $\Gamma_{L(R)} = i\{\nu'_{SL(R)} \Delta_{L(R)}^r \nu'_{L(R)S} - \nu'_{SL(R)} \Delta_{L(R)}^a \nu'_{L(R)S}\}$ [14]. Using the above equations, the conductance at the Fermi energy corresponding to $\theta = 0^\circ, 7^\circ, 11^\circ$, and 15° were computed. The calculation required the determination of the Green’s functions of the sample and the leads. For the size of the system under consideration, the computation of the Green’s functions is not a trivial task. In this work, efficient calculations of the Green’s functions were accomplished using the method of real space Green’s function [15–18]. A similar approach was recently developed by Nardelli [7]. The result of our calculation yields that the conductance (in unit of $2e^2/h$) at E_F changes from 2.0 for $\theta = 0^\circ$, to 1.0 for $\theta = 7^\circ$, to 0.2 for $\theta = 11^\circ$, and to 0.01 for $\theta = 15^\circ$, a change of 2 orders of magnitude altogether, consistent with the experimental observation. Apparently the change from a sp^2 to a sp^3 bonding configuration for atoms in the bending region due to the local deformation induced by the tip had resulted in this drastic reduction in the conductance.

Since the transport properties of a system are mainly determined by electrons (holes) shared by the neighboring atoms in the vicinity of the Fermi energy, we calculated, within the framework of the NOTB, the combined local electron and hole distribution [19] shared by atoms in the central section of the bent NT containing 20 atoms to provide further elucidation of the interplay between the mechanical deformation and the conductance. The results, shown in Fig. 4, give the normalized combined local electron and hole distribution in the vicinity of the Fermi energy in terms of σ —as well as π —bonding character for $\theta = 0^\circ, 7^\circ, 11^\circ$, and 15° , respectively. From Fig. 4(a), it can be seen that the combined local electron and hole distribution for the unbent SWNT is basically composed of π electrons (holes). As the degree of bending increases, the contribution from σ electrons (holes) becomes more and more important [see Figs. 4(b) and 4(c)]. The σ -electron (hole) contribution becomes the dominant one when θ reaches 15° [see Fig. 4(d)]. This result gives a clarifying picture of how the transition from a sp^2 to a sp^3 bonding nature brings about the reduction in the conductance at the Fermi energy.

Our theoretical study has brought out the key feature characterizing the deflection of a SWNT by an AFM tip, namely, the transition from a sp^2 to a sp^3 bonding configuration in the bending region at relatively small bending angles. The resulting drastic reduction in the conductance is the consequence of this change in the bonding nature induced by the action of the tip on the SWNT, rather than the tip itself. This finding elucidates the physics underlying the unexpected electromechanical behavior of the SWNT as it is manipulated by an AFM tip. The identification of the key role played by the local deformation induced by the tip and the unique mechanical property (reversibility)

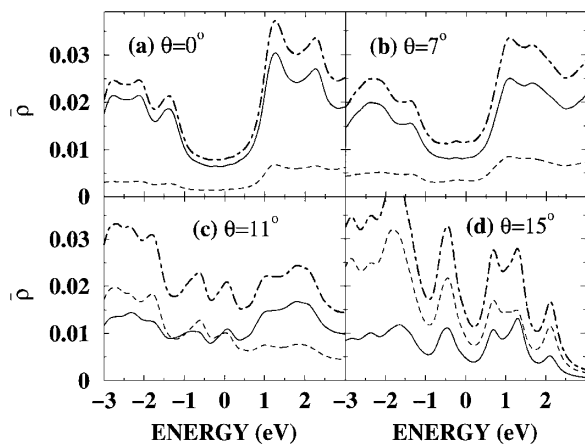


FIG. 4. The average combined local electron and hole distribution per atom, $\bar{\rho}_v$ (see Ref. [19]), in the bending region (central section of the SWNT containing 20 atoms) in the vicinity of the Fermi energy ($E_F = 0$) for (a) $\theta = 0^\circ$, (b) $\theta = 7^\circ$, (c) $\theta = 11^\circ$, and (d) $\theta = 15^\circ$. The dashed line represents the total σ contribution to the combined electron and hole distribution, the solid line the π contribution, and the dot-dashed line the total contribution.

of the SWNT not only point to the possibility that a metallic SWNT may be used as an ultrasmall electromechanical switch, an important ingredient in the development of NEMs, but also hold promises for other applications in nanoscale devices.

This work was supported by NSF grants (DMR-9802274 and ECS-9871947), the Camille Henry-Dreyfus Foundation, and American Chemical Society DARPA/ETO.

- [1] A. Bezryadin, A. Verschueren, S. Tans, and C. Dekker, Phys. Rev. Lett. **80**, 4036 (1998).
- [2] S. Paulson *et al.*, Appl. Phys. Lett. **75**, 2936 (1999).
- [3] V. Crespi, M. Cohen, and A. Rubio, Phys. Rev. Lett. **79**, 2093 (1997).
- [4] C. L. Kane and E. J. Mele, Phys. Rev. Lett. **78**, 1932 (1997).
- [5] M. Nardelli, B. Yakobson, and J. Bernholc, Phys. Rev. Lett. **81**, 4656 (1998).
- [6] A. Rochefort, D. Salahub, and P. Avouris, Chem. Phys. Lett. **297**, 45 (1998).
- [7] M. Nardelli, Phys. Rev. B **60**, 7828 (1999).
- [8] M. Nardelli and J. Bernholc, Phys. Rev. B **60**, 16338 (1999).
- [9] A. Rochefort, F. Lesage, D. Salhub, and P. Avouris, xxx.lanl.gov/cond-mat/9904083 (1999).
- [10] T. W. Tomblor *et al.*, Nature (London) (to be published).
- [11] C. S. Jayanthi, S. Y. Wu, J. Cocks, N. S. Luo, Z. L. Xie, M. Menon, and G. Yang, Phys. Rev. B **57**, 3799 (1998).
- [12] M. Menon, K. R. Subbaswamy, and M. Sawtarie, Phys. Rev. B **48**, 8398 (1993).
- [13] D. Alfonso, S. Y. Wu, C. S. Jayanthi, and E. Kaxiras, Phys. Rev. B **59**, 7745 (1999).
- [14] S. Datta, *Electronic Transport in Mesoscopic Systems* (Cambridge University Press, Cambridge, 1995).
- [15] K. S. Dy, S. Y. Wu, and T. Spratlin, Phys. Rev. B **20**, 4237 (1979).
- [16] S. Y. Wu, Z. L. Xie, and N. Potoczak, Phys. Rev. B **48**, 14826 (1993).
- [17] S. Y. Wu, J. A. Cocks, and C. S. Jayanthi, Phys. Rev. B **49**, 7957 (1994).
- [18] S. Y. Wu and C. S. Jayanthi, Int. J. Mod. Phys. B **9**, 1869 (1995).
- [19] We define

$$\tilde{\rho}_{iv}(E) = \rho(E) \sum_{j(\neq i)} \left| \sum_{\alpha, \beta} \left(-\frac{1}{\pi} \right) \text{Im} R_{i\alpha, j\beta}(E + i\varepsilon) S_{j\beta, i\alpha}^v \right| \left/ \sum_i \sum_{j(\neq i), v} \left| \sum_{\alpha, \beta} \left(-\frac{1}{\pi} \right) \text{Im} R_{i\alpha, j\beta}(E + i\varepsilon) S_{j\beta, i\alpha}^v \right| \right.$$

as the normalized combined electron and hole distribution of bonding nature v ($ss\sigma$, $sp\sigma$, $pp\sigma$, or $pp\pi$) at the i th site. This is accomplished by decomposing $S_{i\alpha, j\beta}$ into its components, $S_{i\alpha, j\beta}^v$. The average combined electron and hole distribution per atom in the central section containing 20 atoms is then calculated according to $\bar{\rho}_v = \frac{1}{20} \sum_i \tilde{\rho}_{iv}$ where i runs through the 20 atoms in the central section of the SWNT. Here, a positive value of $\sum_{\alpha, \beta(v)} \left(-\frac{1}{\pi} \right) \text{Im} R_{i\alpha, j\beta}(E + i\varepsilon) S_{j\beta, i\alpha}^v$ corresponds to the electron distribution, while a negative value corresponds to the hole distribution.